small NANO MICRO

A New Era for Cancer Treatment: Gold-Nanoparticle-Mediated Thermal Therapies

Laura C. Kennedy, Lissett R. Bickford, Nastassja A. Lewinski, Andrew J. Coughlin, Ying Hu, Emily S. Day, Jennifer L. West, and Rebekah A. Drezek**

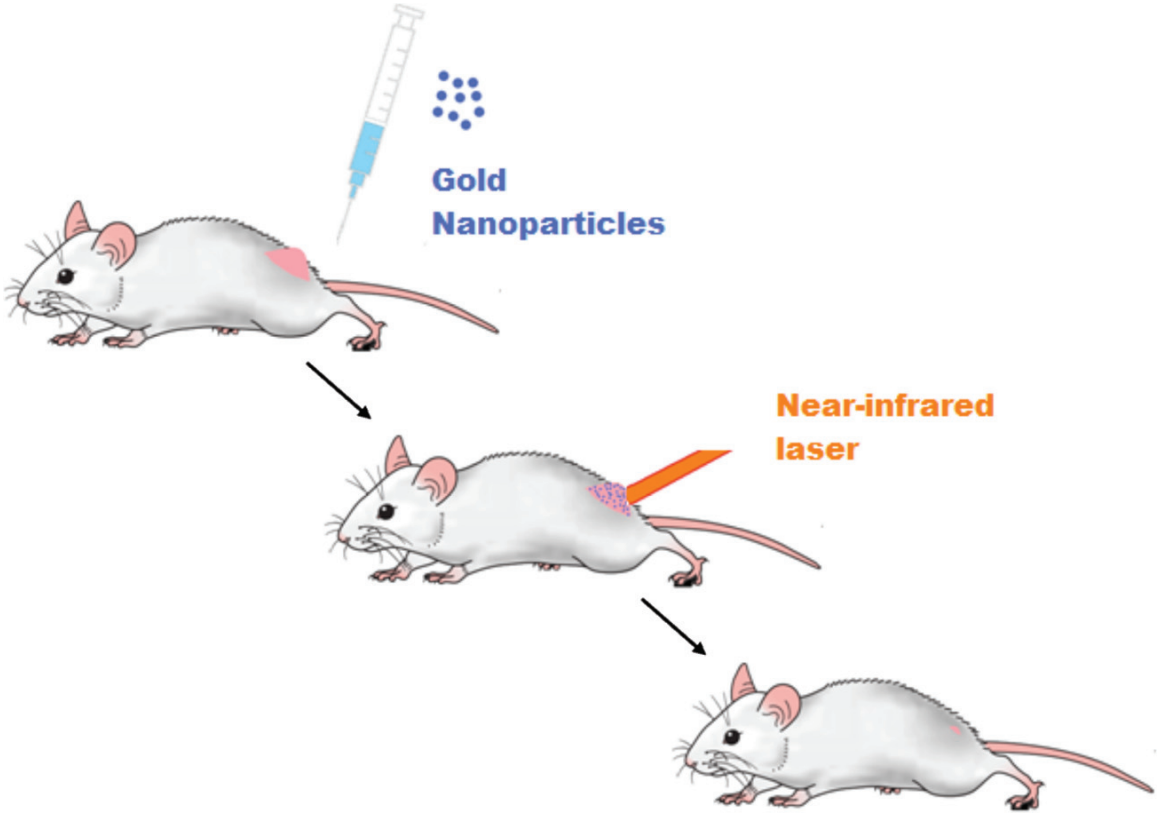

From the Contents

1. Introduction 2
2. Gold Nanoparticle Design for Photothermal Therapy Applications 2
3. Opportunity #1: Methods to Provide Irradiating Energy to the Tumor. 5
4. Opportunity #2: Enhancing In-vivo Delivery and Biodistribution of Gold Nanoparticles 8
5. Opportunity #3: Understanding Impact of Gold Nanoparticle Use In vivo 12
6. Conclusion. 13

Nanotechnology-based cancer treatment approaches potentially provide localized, targeted therapies that aim to enhance efficacy, reduce side effects, and improve patient quality of life. Gold-nanoparticle-mediated hyperthermia shows particular promise in animal studies, and early clinical testing is currently underway. In this article, the rapidly evolving field of gold nanoparticle thermal therapy is reviewed, highlighting recent literature and describing current challenges to clinical translation of the technology.

1. Introduction

In 2010, the National Institutes of Health estimates that more than 1.5 million new cases of cancer will have been diagnosed in the United States, with an overall projected cost of US$263.8 billion.[1] The development of new approaches to improve screening, diagnosis, and treatment of cancer is an area of intensive research spending and has generated numerous innovations that have enhanced the 5-year survival rates of cancer patients.[1] However, these new treatments also contribute to the rising costs of healthcare.[2] To justify these increased costs, state-of-the-art treatments should have enhanced efficacy, decreased invasiveness, and fewer side effects than current cancer therapies. While still in a relatively early stage of technological development, gold-nanoparticle-based diagnostic and therapeutic approaches, particularly those based on gold-nanoparticle-mediated hyperthermia, have shown promise towards achieving these goals.

Gold has been used for the treatment of rheumatoid arthritis for many years,[3] establishing an early precedent for in-vivo use of gold nanoparticles. The wide-ranging utility of gold nanoparticles for medical applications is based largely on the unique and highly tunable optical properties that gold nanomaterials provide. When metallic nanoparticles are exposed to light at their resonance wavelength, the conduction-band electrons of the nanoparticle generate a synchronized oscillation that ultimately terminates in either light scattering or absorption. By carefully designing the size, shape, and composition of gold nanoparticles, the proportion of light scattering relative to light absorption can be optimized for the intended application. Gold nanoparticles are currently being studied for use as imaging contrast agents,[4,5] absorptive heating agents,[6] and as dual imaging and therapeutic agents.[7,8]

The most extensively developed of these potential applications, gold-nanoparticle-mediated hyperthermia, is currently being studied in early clinical trials.[9] To treat a tumor, gold nanoparticles are systemically administered to the subject and allowed to passively localize to the tumor.[10] The tumor is then exposed to an excitation source, such as near-infrared (NIR) laser light,[6] radiowaves,[11] or an alternating magnetic field.[12] The gold nanoparticles absorb the incident energy and convert it into heat, which raises the temperature of the tissue and ablates the cancerous cells by disrupting the cell membrane.[13] The physical heating mechanism of ablative therapies may provide an advantage against chemotherapy-resistant cancers,[14] as well as improved tumor response when combined with chemotherapy and radiation.[15,16]

The continuing evolution of strategies for gold-nanoparticle hyperthermia has generated a rapidly growing body of literature. In this article, we discuss a number of recent notable additions to the field including: 1) the use of small-diameter, near-infrared, tunable gold nanoparticles, which will potentially have enhanced in-vivo access to the tumor interior; 2) delivery strategies focused on increasing the specificity and quantity of nanoparticle delivery to in-vivo tumors; 3) recent developments in computational modeling of thermal therapy, which could be essential for effective clinical translation.

2. Gold Nanoparticle Design for Photothermal Therapy Applications

A diverse range of gold nanoparticles have been explored for use in therapy and imaging applications. Key features to consider when selecting a particle for hyperthermia are the wavelength of maximal absorption, the absorption cross-section, and the size of the particle. In this section, the development of several forms of gold-based nanoparticles used for therapy are discussed, including gold–silica nanoshells, gold nanorods, gold colloidal nanospheres, and smaller-diameter NIR-tunable gold nanocages, gold–gold sulfide nanoparticles, and hollow gold nanoshells.

2.1. Gold–Silica Nanoshells

In 2003, Hirsch et al. were the first to demonstrate photothermal therapy using gold–silica nanoshells.[6] Gold–silica nanoshells, composed of silica cores with a thin overlay of gold, were the first gold nanoparticles easily tunable to the NIR. By varying the size of the silica core and the thickness of the gold shell, the resonance of these nanoshells can span from the visible to the near infrared. Gold–silica nanoshell fabrication is based on seed-mediated growth, where 'seeds' of gold colloid are attached to the silica cores, and additional gold is added for completion of the shell. Similarly to other gold nanoparticles, gold–silica nanoshells have been studied specifically for their potential as imaging contrast agents with darkfield microscopy,[5,11] two-photon microscopy,[17,18] reflectance confocal microscopy,[19] and optical coherence tomography (OCT).[7] In addition to having utility in cancer imaging, nanoshells that are strong absorbers can induce cancer cell death by converting light into heat (**Figure 1**). Silica-based gold nanoshells have been tested in vitro as targeted-therapy probes for human breast,[5,20,21] prostate,[22,23] brain,[24] and liver[25] cancers. In addition, nanoshells have demonstrated in-vivo therapeutic efficacy against xenografted subcutaneous tumors in mice and allografted tumors in dogs.[26,27] The larger size of gold–silica nanoshells as opposed to many other gold nanostructures provides an advantage in scatter-based imaging, but in-vivo delivery may be more challenging than for smaller particles in some applications.

2.2. Gold Nanorods

Gold nanorods, which were developed during the same period as gold–silica nanoshells, are generally smaller than nanoshells. Like gold–silica nanoparticles, gold nanorods

L. C. Kennedy, L. R. Bickford, N. A. Lewinski, Y. Hu, Prof. R. A. Drezek
William Marsh Rice University
Dept. of Bioengineering MS-142
6100 Main St., Houston, TX 77005–1892, USA
E-mail: drezek@rice.edu
A. J. Coughlin, E. S. Day, Prof. J. L. West
William Marsh Rice University
Dept. of Bioengineering
6100 Main St., Houston, TX 77005–1892, USA
E-mail: jwest@rice.edu

DOI: 10.1002/smll.201000134

NANO MICRO small

are easily tuned to the NIR region by simple manipulation of their aspect ratio (length/width) and have been extensively studied for cancer therapy applications. They have the advantages of small sizes (on the order of 10 nm × 50 nm, comparable to gold colloid particles), high absorption coefficients, and narrow spectral bandwidths. Owing to their distinctive rod shape, gold nanorods have two absorption peaks corresponding to the longitudinal and transverse resonances. The transverse resonance occurs at around 520 nm, while the longitudinal resonance can span the visible and NIR wavelengths. Recent studies have investigated the photothermal heating efficiencies of NIR-absorbing gold nanoparticles, and both theoretical and experimental results have shown that nanorods offer a superior absorption cross-section versus gold–silica and gold–gold sulfide nanoparticles when normalizing for particle size differences, as well as heating per gram of gold that is at least six times faster than gold–silica nanoshells.[28–30] However, gold–silica nanoshells have a significantly larger photothermal transduction cross-section when compared to gold nanorods on a per-particle basis.[28] Nanorods have demonstrated success in vivo against oral squamous cell carcinoma and colon cancer xenografted into mice.[31,32] Like gold–silica nanoshells, nanorods can be designed to function as imaging probes, and have been used to enhance the imaging contrast in darkfield microscopy[33] and two-photon microscopy.[34]

A major challenge to the use of gold nanorods for photothermal therapy is their susceptibility to reshaping into gold nanospheres under intense laser illumination, resulting in a loss of the longitudinal NIR resonance. However, an in-vitro study examining the spatial distribution of the reshaping during photothermal therapy of gold nanorods coated with polyethylene glycol (PEG) indicated that, at the laser fluence threshold for gold nanorod conversion, photothermal therapy would still be effective for tumors within 10 mm of the illuminated region.[35] This correlates with the limitations in vivo of NIR laser penetration.

Rebekah Drezek is currently a Professor in the Departments of Bioengineering and Electrical and Computer Engineering at Rice University. She has been on the faculty at Rice since 2002 where she conducts basic, applied, and translational research at the intersection of medicine, engineering, and nanotechnology towards the development of minimally invasive, photonics-based imaging approaches for the detection, diagnosis, and monitoring of cancer.

Jennifer West is the Department Chair and Cameron Professor of Bioengineering at Rice University. Professor West's research focuses on the development of novel biofunctional materials and nanotechnology-based approaches to cancer treatment. In 2000, Professor West, together with Dr. Naomi Halas, founded Nanospectra Biosciences, Inc. to commercialize the nanoparticle-assisted photothermal ablation technology which is now called AuroLase.

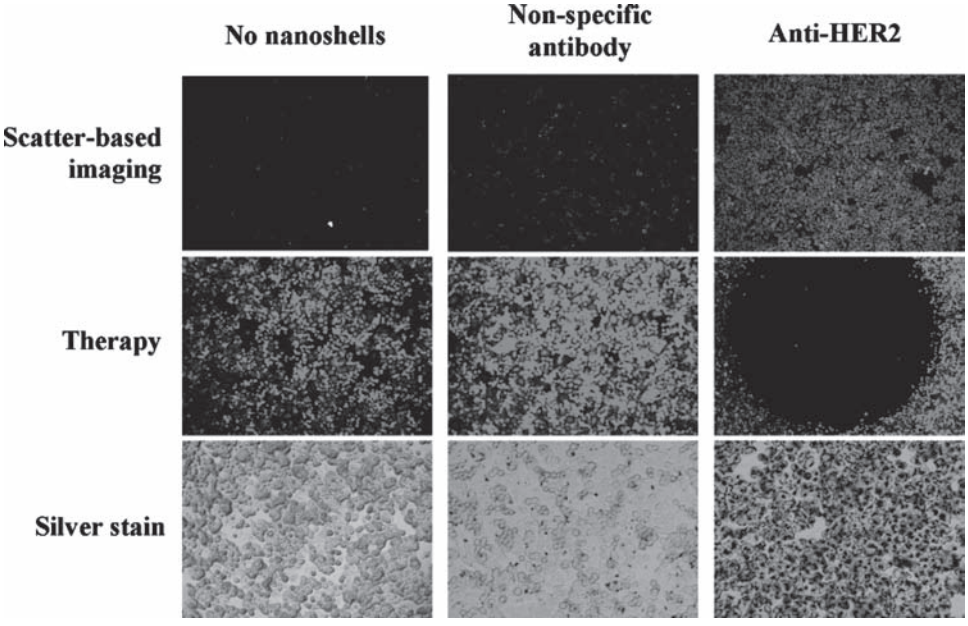

Figure 1. In-vitro imaging and therapy of human epidermal growth factor receptor 2 (HER2)-positive breast cancer cells using anti-HER2-conjugated gold–silica nanoshells. The top row is darkfield microscopy of each treatment group, the middle row is a live stain of the cells after irradiation with NIR light, and the bottom row is a silver stain to show nanoshell binding. The same nanoshells are utilized to both image and ablate the breast cancer cells. Reproduced with permission.[110] Copyright 2005 American Chemical Society.

Photothermal reshaping also strongly depends on the surface conditions of the particle. Heat diffusion through the surface coating can either impede or enhance the reshaping process. Chon et al. implemented a simple heat-diffusion model to estimate the heat relaxation time of gold nanorods encased in silica shells.[36,37] They found that heat dissipation in the silica shell was much faster than the gold-nanorod-reshaping process, resulting in the shell inhibiting nanorod reshaping. In contrast, Horiguchi et al. reported the opposite effect on cetyl trimethylammonium bromide (CTAB) bilayer-coated gold nanorods: CTAB enhanced heat isolation and caused the nanorods to reshape.[38] Additional concerns about CTAB toxicity, discussed later in Section 5.1, suggest the need to further study nanorod surface coatings.

Although gold–silica nanoshells and gold nanorods have proven effective for photothermal therapy due to their easily tunable NIR properties, the size and shape of these nanoparticles impairs efficient tumor delivery in vivo, with less than 5% of the injected dose typically accumulating in the tumor. To address this problem, smaller particles that are tunable to the NIR region are being applied to photothermal therapy applications. In the next subsection, the development of gold–gold sulfide nanoshells, hollow gold nanoshells, and gold nanocages is discussed as an improved, second generation of therapeutic nanoparticles.

2.3. Small NIR-Tunable Gold Nanoparticles

The smaller size of gold–gold sulfide (GGS) nanoparticles, hollow gold nanoshells (HAuNS), and gold nanocages gives a clear delivery advantage for in-vivo photothermal ablation over larger gold nanoparticles. The first example of these smaller gold nanoparticles is gold–gold sulfide nanoparticles, which are smaller than their gold–silica counterparts with total diameters down to 25 nm. These particles are fabricated by the reduction of $HAuCl_4$ using sodium sulfide or sodium thiosulfate, and the synthesis produces two spectral peaks, one at approximately 520 nm due to gold colloid contamination, and one in the NIR region. After synthesis, extensive washing is required to remove contaminating gold colloid from the product. There is some controversy over the exact structure of these particles,[39–41] with some groups describing the nanoparticle as a gold sulfide core coated with a thin gold outer shell, while other groups describe these nanoparticles as aggregates of gold with a thin layer of sulfur on the particle surface. Regardless, these gold nanoparticles have an NIR absorbance that can be utilized for ablative therapy.

A study conducted by Gobin et al. recently examined the potential of gold–gold sulfide nanoparticles for use against prostate cancer in vitro as well as in xenografted tumor mouse models in vivo.[42] Based on Mie scattering theory calculations, Gobin et al. showed that gold–gold sulfide nanoparticles, by their smaller size, have a larger ratio of absorption to scattering than that seen for gold–silica nanoshells (98% absorption for gold-gold sulfide nanoparticles versus 70% absorption for gold–silica nanoshells). Using particles with core diameters ranging from 30–40 nm and a shell thickness of 3–6 nm, cancer cells were successfully ablated in regions where the NIR laser and GGS nanoparticles were simultaneously applied. For an in-vivo comparison of gold–gold sulfide and gold–silica nanoshells, both particle types were stabilized with PEG and injected intravenously into tumor-bearing mice. After allowing the particles to accumulate at the tumor site over a 24 h period, the tumors were exposed to NIR light. Results showed that ≈71% of the mice survived for the duration of the study (8 weeks post-injection) for the gold–gold sulfide group, while ≈82% survived for the gold–silica nanoshell group. However, when gold–gold sulfide nanoparticles were allowed to accumulate in tumors for 48 h, the survival of the mice increased to 82%. This suggests that the longer circulation time of the GGS nanoparticles caused maximal accumulation to occur at later timepoints than gold–silica nanoshells, which have optimal tumor accumulation time of 24 h.

Another type of gold nanoparticle explored for potential cancer therapy is the hollow gold nanoshell. As the name implies, these particles consist of a hollow center with a thin gold shell and can have a total diameter on the order of 30 nm, with a shell thickness of ≈8 nm. By fabricating cobalt or silver nanoparticles and then oxidizing this template material with the addition of chloroauric acid, a thin shell of gold with no solid material at the core can be created.[43,44] In studies conducted by Li et al., HAuNS conjugated to anti-Epidermal Growth Factor Receptor (EGFR) antibodies were used to target and ablate EGFR-overexpressing cells,[45] and hollow gold nanoshells conjugated to a melanocyte-stimulating hormone (MSH) analog were subsequently used in vivo to ablate xenografted subcutaneous murine melanoma tumors.[46] As an added advantage, the hollow core of these nanoshells can be used as a delivery vehicle for drugs or enzymes.[47]

The final group of small diameter NIR gold nanoparticles discussed here are gold nanocages. These particles are synthesized by first creating template silver nanoparticles and then replacing the silver with gold in a manner analogous to the HAuNS.[48] By adjusting the wall thickness of the nanocages, the absorption peak can be varied from 400 to 1200 nm, with an edge length range of 30 to 200 nm. Gold nanocages have been examined as contrast agents for OCT[49] and as human epidermal growth factor receptor (HER)2-targeted therapeutic agents for HER2-overexpressing breast cancer cells.[50–52] Chen et al. performed a successful in-vivo study using gold nanocages to ablate murine models with subcutaneous glioblastoma.[53] Twenty-four hours after mice were treated with gold nanocages in tandem with near-infrared laser therapy, results showed that tumor metabolism had declined 70%, unlike the saline-injected mice, which showed no difference in metabolic activity on positron emission tomography.

2.4. Gold Colloidal Nanospheres

The final group of gold nanoparticles discussed for hyperthermia applications are gold colloidal nanospheres. Previously, these solid gold spheres were solely investigated for their use as imaging probes.[4,54,55] However, the small size and relatively simple synthesis of these particles make them

small NANO MICRO

appealing for hyperthermia applications. A key disadvantage of these particles is their absorbance peak, which is in the visible region at around 530 nm. This wavelength is outside the NIR window, presenting a difficulty for in vivo studies, as discussed in detail in Section 3.

Photothermal therapy with gold nanospheres has been explored in both the visible[8,56,57] and near-infrared[58] wavelength regions. El-Sayed and colleagues first reported the use of gold colloidal nanospheres for the imaging and therapy of oral cancer cells in vitro using a continuous argon laser at 514 nm, which is closely coincident with the peak absorbance of 40 nm particles.[57] Compared to normal, noncancerous cells, it was demonstrated that cancerous cells targeted with nanoparticles were destroyed with 2–3 times lower laser power.

To shift the absorbance of gold colloidal nanospheres away from the visible region and into the NIR, the nanoparticles can be aggregated or clustered together in close proximity. El-Sayed et al. used a short-pulsed, NIR laser on small gold aggregates formed from 30 nm gold colloidal particles to selectively ablate oral cancer cells.[58] By operating in the NIR, the laser power needed to kill the cancer cells was approximately 20 times less than that needed to destroy normal cells. Alternatively, a similar result has been achieved using gold nanoclusters and photothermal microbubbles (PTB). Here, non-aggregated gold colloid is incubated with cancer cells and subsequently internalized via endocytosis. The nanoparticles are in close proximity to each other within the cell endosome, creating a shift in the nanoparticle absorbance to the NIR.[59] Through the use of laser pulses in either the visible[60,61] or NIR[59] regions, vapor bubbles ranging from 10^{-8} to 10^{-4} m[61] can be formed around the nanoclusters. These PTB are the mechanism by which the cells are irreversibly damaged. Moreover, these vapor bubbles are detectable throughout their lifespan with a photothermal microscope, presenting the ability to both image and treat simultaneously.[62] The potential of this unique theranostic system has been demonstrated for both leukemia[60,61] and breast cancer cells.[59]

2.5. Selecting a Therapeutic Gold Nanoparticle for Translation

With the preliminary successes of gold-nanoparticle hyperthermia in animal studies, attention is now being turned to addressing considerations important for expanding the use of this technology. The first decision is the selection of the gold nanoparticle variant. The efficiency with which a nanoparticle absorbs and scatters light is an essential parameter to consider when choosing a particle for use in an application. From a photothermal-therapy perspective, the absorptive cross-section is an important variable. Calculating the absorption cross-section of gold-based nanoparticles can be achieved by using Mie-based theory or numerical methods such as a discrete dipole approximation.[63–66] Particle design is optimized by maximizing the absorption efficiency at a desired wavelength in a specific surrounding medium in order to achieve a maximum particle temperature and surface heat flux.[66,67] Cole et al. compared the photothermal efficiencies of gold–silica nanoshells, gold–gold sulfide nanoshells, and gold nanorods.[28] They found that the photothermal transduction efficiencies, defined as the portion of incident light being converted into photothermal power by the nanoparticle, varied by less than a factor of three between the different particles studied.[28] This finding suggests that no particular nanoparticle configuration has significant therapeutic advantage over the others.

While there has been significant focus to date on identifying ideal gold nanoparticle configurations for photothermal therapy, there are several additional promising research avenues for further optimization of the technology. The use of NIR light and nanoparticle absorbers in photothermal therapy offers critical advantages, particularly in protecting healthy tissue from thermal damage. However, solid tumors can occur within the body at depths greater than 1 cm, which is beyond the penetration of NIR light in tissue. In these cases, fiber-optic probes often can be used to deliver light. In addition, the use of alternative irradiation modalities is an area of recent significant research activity and may be particularly useful for treating tumor locations that are difficult to access from the surface or through interstitial fiber-optic devices. A second area of current research activity is the optimization of the delivery and biodistribution of gold nanoparticles in vivo. To ensure therapeutic success, maximal gold nanoparticle accumulation in the tumor is highly desirable. Furthermore, minimization of gold-nanoparticle accumulation within nontarget organs such as the liver and spleen is ideal. The use of smaller nanoparticles enhances the blood half-life and improves tumor accumulation and specificity. However, it is likely that additional modifications beyond size optimization would be useful to further improve nanoparticle biodistribution, and this has become an area of expanding research. A final area of current research activity is the identification of any impact of the long-term presence of gold nanoparticles in vivo. Relatively short-term studies have been performed to date with highly encouraging results. The remaining sections of this review will focus on discussing these areas of current research activity and future opportunity.

3. Opportunity #1: Methods to Provide Irradiating Energy to the Tumor

The penetration depth of NIR light in tissue is a key limiting factor in the expansion of gold-nanoparticle hyperthermia. The selection of irradiation modality for gold-nanoparticle hyperthermia is a balance of three factors: sufficient depth penetration to reach the nanoparticle-laden cancerous tissue, extraneous heating of healthy tissue due to energy absorption by tissue chromophores and off-target nanoparticles, and the properties of the chosen therapeutic nanoparticles. NIR light is generally favored in gold-nanoparticle-therapy studies due to its low absorbance by tissue chromophores, which prevents it from damaging healthy tissue. For successful cancer ablation, the tissue must be heated to a minimum temperature for a minimum duration of time to induce tumor cell death. If the irradiating energy cannot reach the depth of the nanoparticles at an adequate intensity, cancerous tissue may be heated insufficiently and survive. Cytotoxic effects have been demonstrated in cells maintained at 42 °C for 1 h, and this duration

can be shortened to 3–4 min by using higher temperatures of 70–80 °C.[68–71] At the molecular level, hyperthermic effects can be seen as changes to the cytoskeletal structure, cell membrane rupture, protein denaturation, impairment of DNA and RNA synthesis, and programmed apoptosis.[69,70] Three possible options of irradiating modality are discussed in the following subsections: NIR light, radiofrequency ablation, and magnetic fluid hyperthermia.

3.1. Near-Infrared Photothermal Ablation

NIR laser light is ideal for in-vivo hyperthermia applications because of its low absorption by tissue chromophores such as hemoglobin and water. The absorption coefficient of these tissue chromophores is as much as two orders of magnitude greater in the visible region (400–600 nm) as compared to the NIR region (650–900 nm).[72,73] Gold-nanoparticle-mediated photothermal therapies are predominantly designed to operate in this window of wavelengths (the "NIR window") to minimize attenuation of the energy resulting from undesired light–tissue interactions, and to prevent undesirable and damaging heating of healthy tissue. Upon tumor laser irradiation, NIR light is absorbed by the nanoparticles and heat dissipation is generated as a consequence of electron–phonon interactions. Hirsch et al. demonstrated a 4–6 mm depth of thermal damage in mice with subcutaneous tumors after intratumoral injection of gold–silica nanoshells and subsequent continuous-wave NIR light exposure (λ = 820 nm, 4 W cm^{-2}, 5 mm spot size, 6 min maximum exposure time).[6]

One alternative that has been suggested to enhance NIR therapy is the use of a pulsed-mode laser instead of a continuous-wave laser. Pulsed lasers permit more efficient photothermal conversion because of lapses between the pulses, allowing additional time for electron-phonon relaxation. Using folate-conjugated gold nanorods bound to a folate-overexpressing cell line, membrane blebbing was demonstrated after exposure to a femtosecond-pulsed NIR laser at a power as low as 0.75 mW in vitro, while a continuous-wave laser required a power of 6 mW to achieve the same effect.[13]

The in-vivo penetration depth of NIR light is dependent on a variety of factors, including the degree of light scattering and absorption within tissue.[6,74] The heating of tissue is dependent on the NIR light intensity at a given point, the absorptive cross-section of the gold nanoparticle, the distribution and concentration of nanoparticles within the tissue, and the degree of NIR light absorption by the tissue chromophores. Accurately modeling the heating profile of nanoparticle-laden tissue is very important for optimizing thermal ablation in solid tumors. In a patient, the distribution of nanoparticles within the tumor, placement and orientation of NIR light, and any variation in the optical and thermal properties of the tumor tissue will affect tumor heating. Simulations of nanoparticle-laden tissues can be constructed using a variety of analytical and numerical approaches, such as light- and heat-diffusion theory, computational electromagnetic methods, and stochastic ray tracing.[75–78]

Elliott et al. modeled the laser fluence and temperature distribution of tissue phantoms embedded with gold–silica nanoshells of various optical densities (ODs) and demonstrated a maximum temperature change of 16 °C for the 0.55 OD phantom and 21 °C for the 0.65 OD phantom using a 3 min 1.5 W laser irradiation.[77] In a later paper, they described an analytical model developed using Green's function method to solve the heat-diffusion equation that calculated the spatiotemporal thermal profile for phantoms with higher concentrations of nanoshells more accurately than the optical-diffusion approximation.[75,76] Modeling of higher concentrations of nanoparticles is important due to the nature of gold nanoparticle distribution within the tumor. NIR narrow-band imaging has revealed that gold nanoparticles tend to accumulate in highly concentrated pockets within the tumor, and that the gold nanoparticle distribution is very nonuniform.[79] The lack of uniformity and the high concentration of nanoparticles in certain regions influences the spatial distribution of tumor heating and provides challenges in modeling ablation of tissue undergoing gold-nanoparticle hyperthermia. These in-vitro models provide the theoretical basis for developing in-vivo simulations. However, these simple models do not account for variations in the tissue optical properties that are expected in vivo.

Simulations based on nanoparticles distributed in tissue extend models to a more realistic medium. Vera et al. investigated the effects of gold–silica nanoshell concentration, laser power, and laser arrangement on the thermal profile of gold-nanoshell-laden human tissue from different organs ex vivo.[78] For this analysis, the optical and thermal properties of the tissue were extrapolated from previous studies at room temperature, and assumed to remain constant during heating. When using a single, externally placed laser for therapy, they found that undesired overheating in one region could occur while leaving the rear region under-heated. It was hypothesized that this uneven heating could be mitigated by the use of an opposing dual-laser heating configuration. For in-vivo applications, this would mean the minimally invasive placement of a fiber-optic probe within the tumor to conduct NIR light, similar to the work done by Schwartz et al. in their study of nanoshell-mediated therapy for tumors in the brain.[27] To optimize probe placement, simulations could be used to select a location that would give maximal heating by accounting for variations in the optical and thermal properties of tissue.

A recent study by von Maltzahn et al. demonstrated the potential of using computational simulations to model in-vivo thermal therapy and assist in understanding the effect of nanoparticle concentration on heating in vivo. An X-ray CT scan was utilized to characterize the distribution of intratumorally and intravenously administered PEGylated nanorods within the tumor.[30] The high absorption efficiency of the gold nanorods in both the X-ray and NIR regions enabled real-time visualization and therapy, and shows promise towards optimizing therapies to match an individual patient's nanoparticle tumor distribution.[30]

The limited penetration of NIR light in tissue confines gold-nanoparticle hyperthermia to solid tumors that are either directly accessible, such as skin cancer, or can be indirectly accessed via endoscopy or interstitial fiber-optic placement. For cancers that cannot be accessed via any of these methods, alternative irradiation methods may provide

small NANO MICRO

an avenue for hyperthermia treatment. We discuss two of these methods in the following subsection: radiofrequency ablation and magnetic fluid hyperthermia.

3.2. Alternatives to NIR Light

Radiofrequency ablation (RFA) was first established in the early 1900s as a method for cauterizing blood vessels during surgery. However, it was not explored for oncologic hyperthermia applications until the early 1990s. Conventional RFA treatments require an invasive procedure to place electrodes within the tumor. Tumor shrinkage occurs as a result of radiowave-induced vibrations of ions within tumor tissue, which give rise to friction and heat.[80] Radiowaves have significantly better penetration of tissue than NIR light, making RFA appealing for deeper solid tumors;[81] however, in exchange for the greater depth of penetration, there is a greater attenuation of the energy by tissue. Adding a mediating absorptive agent, such as gold nanoparticles, increases the specificity of RFA treatments, protects normal tissue by lowering energy requirements, and may decrease the need for invasive electrode placement.[11]

RFA has shown promise in creating thermal lesions within liver tumors, and the addition of absorptive mediators, such as gold nanoparticles[11,82] or carbon nanotubes,[83] has been found to enhance this effect. In mice bearing subcutaneous tumors treated with RFA, the temperature increase within the gold-nanoparticle-treated tumors averaged 10 °C compared to 4 °C among control tumors injected with sterile water.[82] In addition, histopathologic features characteristic of thermal injury, such as hyperchromatism and cellular fragmentation, were noted within the treatment group.[82] Gannon et al. also studied nanoparticle-assisted radiofrequency ablation of liver tumors using single-walled carbon nanotubes in New Zealand white rabbits with successful results.[83]

Magnetic fluid hyperthermia (MFH) is another form of nanoparticle-assisted thermal therapy currently under investigation. This form of thermal therapy utilizes magnetically susceptible particles in suspension to emit heat in the presence of an alternating-current (AC) magnetic field. The magnetic energy of the external alternating field is converted to internal energy within the nanoparticles and subsequently released as thermal energy through Brownian and Néel relaxations. Superparamagnetic particles are known to undergo this conversion at lower field strengths, and iron oxide nanoparticles are most commonly used owing to their established biocompatibility and the availability of methods for chemical modification.[84] Since alternating magnetic fields do not tend to be susceptible to attenuation by tissue, the main advantage of MFH compared to other methods of heat delivery lies in its ability to treat deeply embedded tumors. In addition, nanoparticles used for MFH can also be used as contrast agents for magnetic resonance imaging, presenting a clear theranostic advantage.

Clinical trials using iron oxide nanoparticles for MFH of cancer are currently being performed by MagForce Nanotechnologies AG. Utilizing these particles with MFH has met with clinical success in a prostate cancer patient.[12] In this feasibility study, it was demonstrated that MFH could produce temperatures in the tumor sufficient to induce thermal insult following direct intratumoral delivery of iron oxide nanoparticles.[12] More recently, MFH has been applied to the treatment of glioblastoma.[85] The investigators delivered iron oxide nanoparticles directly to brain tumors in 14 patients, who were then treated with a combination of radiation and MFH without any significant adverse responses to the therapy.[85] These results are encouraging, and further development of MFH could yield an effective alternative to current treatment options for advanced cancers.

Although MFH has not yet been applied using gold nanoparticles, a number of composite particles using gold and a magnetic material have been developed.[86–89] These composite particles present possibilities for either NIR photothermal ablation and optical imaging, or for MFH and MR imaging. Larson et al. synthesized γ-Fe_2O_3–Au core–shell nanoparticles and demonstrated their use as magnetic resonance imaging (MRI) contrast-enhancing agents and as NIR-absorbing agents for the targeted photothermal ablation of cancer in vitro.[86] Although the absorbance spectra for these particles did not show a pronounced peak within the NIR region, clustering of anti-EGFR-conjugated nanoparticles along cell surfaces allowed for sufficient heating to induce cancer cell death in vitro using a pulsed-mode laser at 700 nm. Similarly, Kirui et al. demonstrated photothermal therapy and MRI potential with 25 nm dumbbell-shaped gold–iron oxide aggregates.[90] Shah et al. used gold–iron oxide nanoparticles to enhance the ex-vivo photoacoustic imaging contrast, used to guide photothermal cancer therapy.[91] In this study, they incorporated a simple model to relate the pressure change to the temperature rise caused by the energy absorption of the gold nanoparticles. With further development, composite gold–magnetic particles may represent a versatile, clinically relevant nanoparticle with sufficient flexibility to permit either photonically or magnetically controlled tumor ablation and imaging. This type of nanoparticle may represent the future of gold nanoparticle theranostics.

The successful photothermal ablation and imaging of a tumor requires both sufficient penetration of the excitation energy and adequate accumulation of the gold nanoparticles within the tumor. NIR light has an advantage over other wavelengths because of its maximal transmissivity in tissue, which minimizes the heating of non-target tissues. Fiber-optic probes provide simple, facile, and inexpensive light delivery to deeper tissue and the development of alternative irradiation modalities further expands accessible regions. With continuing research into this area, the depth of a tumor will not impede treatment using gold-nanoparticle-photothermal therapy. Another key issue that affects the efficacy of gold-nanoparticle-hyperthermia treatments is the delivery of gold nanoparticles to the tumor. Gold nanoparticle tumor accumulation is typically a small percentage of the total injected dose, with the majority of the injected dose amassing in non-target organs such as the liver and spleen. In **Figure 2**, mice treated using intratumorally administered nanoparticles have smaller tumors at 11 days post-treatment than mice treated

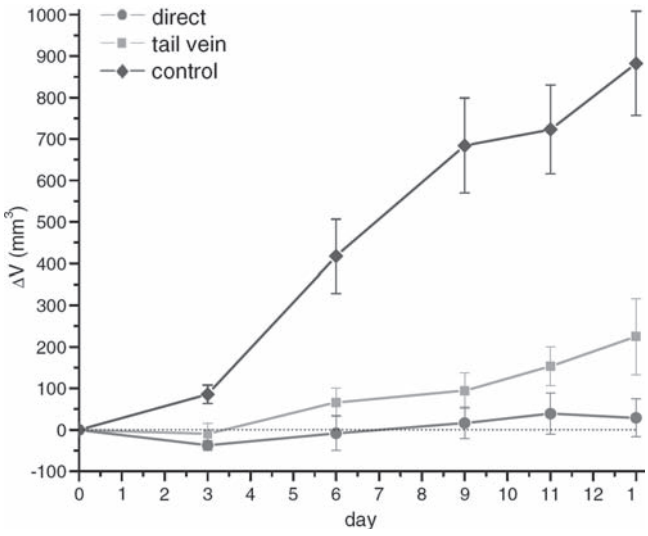

Figure 2. Tumor volume change over time following NIR light treatment for mice receiving phosphate buffered saline (PBS, control), intratumoral injection of PEGylated gold nanorods (direct), and systemically injected, PEGylated gold nanorods (tail vein). Mice receiving treatment experienced less tumor growth than the control mice. However, mice receiving directly injected nanorods had improved survival rates beginning 11 days post-treatment, suggesting that mice injected via tail vein had a lower tumor concentration of gold nanorods. Reproduced with permission.[31] Copyright 2008 Elsevier.

using intravenously delivered nanoparticles, although this difference never achieves statistical significance at a 5% level.[31] It is suggestive, however, that nanoparticle delivery is an important factor for the success of therapy. The next section addresses the issues of gold nanoparticle biodistribution and tumor delivery.

4. Opportunity #2: Enhancing In-vivo Delivery and Biodistribution of Gold Nanoparticles

Initial testing of gold-nanoparticle therapy in vivo used direct intratumoral injection.[6] While this method was very successful in the subcutaneous tumors studied, the lack of clinical applicability led to a rapid transition to using systemic injection for delivery of the nanoparticles. Nanoparticle accumulation within the tumor after systemic administration is typically attributed to the enhanced permeability and retention effect. After injection, nanoparticles passively localize to the tumor by passing through the fenestrations of the angiogenic tumor vasculature, which is malformed compared to normal blood vessels, and thus more permeable. However, the passage of nanoparticles through these fenestrations is dependent on both the size of the particles and the stage of tumor development; early-stage tumors have smaller fenestrations and thus lower nanoparticle accumulation.[92]

To optimize therapeutic success and minimize long term side effects, in-vivo nanoparticle accumulation would be limited to the cancer alone. In addition, to optimize the diffusion of heat, the nanoparticle distribution throughout the tumor should also be concentrated and homogeneous. In reality, nanoparticle accumulation is spread throughout the body, and the nanoparticles tend to concentrate around the tumor vasculature. In the following subsections, we will discuss the biodistribution of gold nanoparticles within a mouse model and the strategies that have been proposed to enhance gold nanoparticle delivery.

4.1. Gold Nanoparticle Biodistribution in Mice

Nanoparticle biodistribution is influenced by the size and surface characteristics of the nanoparticle. Rapid clearance from the blood hinders nanoparticle delivery to target sites, and, consequently, most nanoparticles developed for medical applications are coated with chains of polyethylene glycol (PEG). Pharmaceuticals, such as peptide drugs, are coated with PEG for similar reasons.[93,94] The addition of PEG increases the hydrodynamic particle size, which prevents filtration by excretory organs, sterically hinders nonspecific binding of proteins to the particle surface, and delays recognition of the particles by the reticuloendothelial system (RES).[95] This ultimately increases the circulation time of the particles.

Zhang et al. found that after intravenous administration to mice, 20 nm PEG-coated (PEG molecular weight = 2000 g mol^{-1}) gold colloidal nanospheres had slower clearance, less uptake by RES cells, and higher accumulation in the tumor compared to 40 and 80 nm particles.[95] This contrast was attributed to both nanoparticle size and PEG-layer density differences, as the 80 nm particles were found to have lower PEG density than the 40 nm particles. Similarly, Terentyuk et al. compared 15 and 50 nm PEG-coated gold colloidal nanospheres with 160 nm PEG-coated gold–silica nanoshells in vivo, and higher blood concentrations of gold were found after 24 h for the 15 nm gold nanoparticles as compared to the 50 nm gold colloid and 160 nm nanoshells.[96] Most recently, a systematic study conducted by Perrault et al. evaluated the effect of nanoparticle size and PEG coatings of different molecular weights on blood circulation time, showing that increased blood half-life by the addition of PEG was more prominent in smaller versus larger total diameter particles (**Figure 3**).[97] Notably, 20–50 nm particles have more effective PEG coverage and consequently longer blood half-lives, and they are also in the optimal size range for cellular uptake.[98]

The intratumoral distribution of nanoparticles is also influenced by the size of the nanoparticles. Perrault et al. observed that particles in the 100 nm range stay within the perivascular regions of the tumor, while smaller particles (<60 nm) have more success dispersing throughout the tumor (**Figure 4**).[97] Tunnell et al. also observed non-uniformity of the nanoparticle distribution when visualizing the placement of gold–silica nanoshells in relation to tumor blood vessels (Figure 4), and observed that the nanoshells remained in close proximity to the vasculature.[79] An additional property of gold nanoparticles that has been suggested to affect tumor distribution is surface charge. Kim et al. performed a study looking at positively and negatively charged gold nanoparticles in tumor cylindroid models, and found that positively

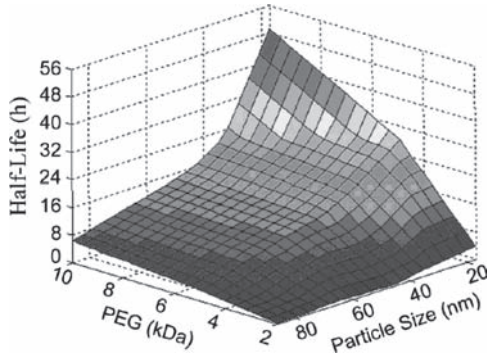

Figure 3. Effect of PEG chain length and particle size on the blood half-life of gold colloidal nanospheres. Smaller gold nanoparticles demonstrate increased PEG surface density, which correlates with an increased half-life in the blood. Reproduced with permission.[97] Copyright 2009 American Chemical Society.

charged nanoparticles were efficiently endocytosed by tumor cells, but negatively charged nanoparticles spread throughout the bulk of the tumor more rapidly.[99] Thus, tumor accumulation and distribution depend on striking an effective particle size and surface charge balance.

For tumor applications, biodistribution studies have primarily looked at gold nanoparticles coated with PEG in subcutaneous tumor mouse models. A comparison of delivery between different types of nanoparticles proves challenging from the current literature because of the lack of standardization of the gold measurements presented. Some groups display their data as a ratio of the gold found in the organ versus the gold found in the tumor, others as a percentage of the injected dose, and still others as a percentage of the injected dose normalized to the lyophlized tissue mass. However, it is clear from the data that the liver and spleen receive significantly more gold than the tumor site. James et al. studied gold–silica nanoshells (130 nm) after intravenous administration to mice and noted a peak tumor accumulation of the nanoshells at 24 h.[100] The concentration of gold reported in the liver and spleen tissue at 24 h was 20–25× the gold concentration observed in the tumor, indicating that <5% of the injected dose was delivered to the tumor (**Figure 5**).[100] Similarly, Dickerson et al. compared direct intratumoral versus systemic injection for PEG-coated nanorods (12 nm × 50 nm, aspect ratio = 4).[31] For the directly injected particles, NIR transmission images showed a measured extinction 4.35 times higher compared to the saline control 2 min post-injection, with no changes over several hours. For the systemically administered nanorods, a maximal tumor accumulation was seen 24 h post-injection, with an extinction that was 2.00 times greater than the saline control. This indicates that tumor accumulation occurs when using the systemic injection method, but a significant loss of particles to other anatomical locations also occurs (Figure 2).

One difference between the biodistribution of gold–silica nanoshells and gold nanorods is the ratio of spleen:liver accumulation. While gold–silica nanoshells show more accumulation in the spleen than liver,[100] gold nanorods show a greater accumulation in the liver than spleen.[32,101] To compensate for this, Akiyama et al. presented data suggesting that increasing the PEG:Au molar ratio to 1.5 or above for similarly sized gold nanorods can reduce the amount of gold seen in the liver and the spleen when compared to the tumor.[102] However, for this study, organ resection was performed at a 72 h time point instead of a 24 h time point, and the difference in liver and spleen accumulation seen could simply be a reflection of increased clearance time instead of decreased delivery.

Gold nanoparticle liver accumulation is often observed irrespective of particle size.[100,101,103–108] De Jong et al. found that 10, 50, 100 and 250 nm gold nanoparticles all accumulate in the liver, and suggested that this was caused by the high perfusion of blood through this organ.[105] However, both bare and PEG-coated gold nanoparticles can be found localized within Kupffer cells, which are phagocytic cells present in the liver, suggesting that phagocytic uptake plays a significant role in the large gold accumulations seen in the liver.[104,107,109]

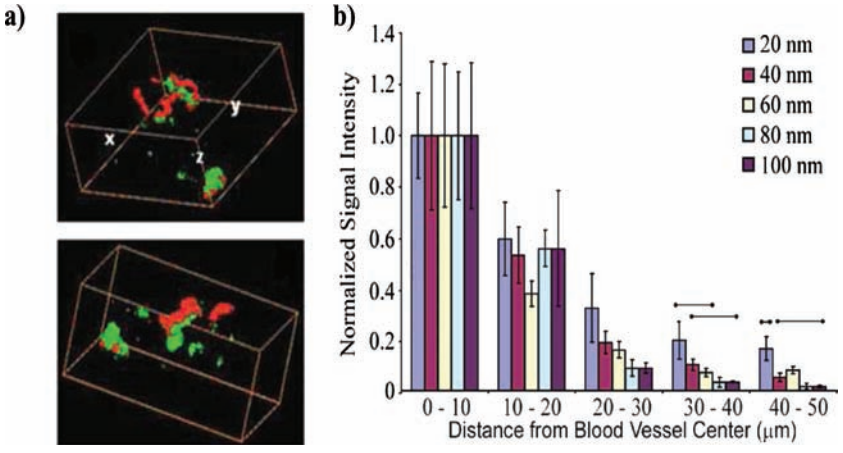

Figure 4. a) Gold-silica nanoshell distribution within a tumor in vivo. A two-photon confocal image was taken of a subcutaneous colon cancer tumor in a mouse model. Tumors were excised after accumulation of nanoshells and immediately imaged. Tumor blood vessels labeled with fluorescein (red) and nanoshells (green) were imaged utilizing their two-photon characteristics. The perivascular relationship of gold—silica nanoshells (green) to the tumor vasculature (red) is clearly evident. Reproduced with permission.[18] Copyright 2008 Optical Society of America. b) Gold colloidal nanosphere distribution with respect to distance from tumor blood vessels by densitometry analysis of tumor sections. Reproduced with permission.[97] Copyright 2009 American Chemical Society.

The large size of nanoshells and the shape of nanorods contribute to difficulties in tumor delivery and biodistribution. However, these challenges can be mitigated by the creation of nanoparticles that are more compact with smaller diameters, such as gold–gold sulfide nanoshells and gold nanocages. A recent in-vivo study by Gobin et al. compared gold–gold sulfide nanoshells (total diameter = 35–55 nm) to conventional gold–silica nanoshells (total diameter = 120–160 nm).[42] Biodistribution studies showed that at 24 h a greater number of gold–gold sulfide nanoshells localized to the tumor versus the spleen and liver as compared with

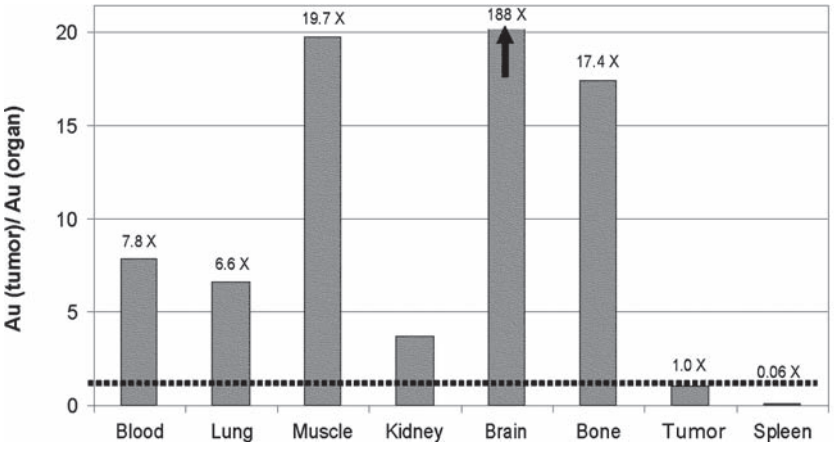

Figure 5. Biodistribution of gold nanoparticles in a mouse model following systemic administration via the tail vein. All organs show less accumulation than the tumor with the exception of the spleen, which has 16.7 times the gold of the tumor. Reproduced with permission.[100] Copyright 2007 Springer.

gold–silica nanoshells, and the gold–gold sulfide nanoshells had a significantly greater blood half-life as compared to the gold–silica nanoshells.[42] A study of gold nanocages in vivo also showed an increased tumor delivery of 5.7% injected dose per gram of lyophilized tissue at 96 h.[53] However, although the smaller size of the nanocages improved the delivery yield to the tumor, the tumor distribution of the nanocages in relation to the tumor vasculature is not substantially changed from that of the larger nanoparticles. Investigators also observed that the nanoparticles were predominantly located at the tumor periphery rather than the tumor core, likely due to superior vascularization at the tumor edges.[53,97]

While, the smaller size of the gold–gold sulfide nanoshells and gold nanocages appears to improve both the tumor delivery and biodistribution, it is still less than ideal. Redirecting nanoparticles from the liver and spleen to the tumor would improve the chance of therapeutic success, reduce the risk of undesired side effects, and permit improved differentiation between metastases and healthy tissue during imaging. The next subsection focuses on strategies designed to improve gold nanoparticle tumor accumulation and retention, as well as the gold nanoparticle biodistribution. The first group of these strategies focuses on the addition of surface molecules such as tumor-specific markers to enhance nanoparticle tumor retention and decrease nanoparticle accumulation in nontargeted sites. The second group of strategies utilizes acellular and cellular vehicles to transport nanoparticles to their destinations.

4.2. Strategies to Enhance Tumor Accumulation of Gold Nanoparticles

To optimize the delivery of gold nanoparticles and enhance ablative therapy, two types of strategy have been reported in the literature. The first strategy utilizes the addition of markers to the nanoparticle surface to increase the nanoparticle specificity for a particular cancer and to bind the nanoparticle directly to the cancer-cell surface, which has advantages for both therapy and imaging. The second strategy utilizes larger particles or cells to target the tumor, with the rationale that these larger vehicles may not accumulate at such a high rate in nontarget sites such as the liver. These vehicles would carry the therapeutic nanoparticles to the tumor site, where they could then diffuse from the tumor vasculature into the tumor body. The goal of both of these strategies is to increase nanoparticle accumulation in the tumor tissue to enhance thermal ablation.

4.2.1. Nanoparticle Surface Modifications

One advantage of gold nanoparticles is the simplicity of modifying the nanoparticle surface. By adding an antibody or other small molecule to the nanoparticle surface that corresponds with the targeted cancer, it has been suggested that the specificity of tumor accumulation and tumor cell-specific binding could be increased. There have been many in-vitro studies supporting this hypothesis. Loo et al. were the first to demonstrate increased specificity of binding, dark-field imaging, and photothermal therapy in vitro using gold–silica nanoshells modified with an antibody to the HER2 receptor, which is overexpressed in some breast cancers (Figure 1).[20,110] The El-Sayed group subsequently demonstrated in-vitro cancer ablation using anti-EGFR-conjugated gold nanorods.[33,71] The specificity of antibody-targeting for therapy has been demonstrated with several other antibodies in vitro, including antibodies for acute lymphoblastic leukemia, *Pseudomonas aeroginosa*, and medulloblastoma.[24,61,111] Similar to tumor-specific antibodies, small molecules specific for cancer cells have also been added to the surface of gold nanoparticles based on the hypothesis that these molecules will diffuse through tissue more efficiently than antibodies because of their small size. Using folate-conjugated nanorods, Tong et al. demonstrated that more laser power was required to kill cells with internalized nanorods versus cells with surface-bound nanorods in vitro.[13] This was also demonstrated using gold nanorods conjugated to modified deltorphin peptide.[112] Other groups have used targeting moieties such as bombesin to specifically target breast and prostate cancers for imaging,[113] arginine-rich peptides to promote specificity via nanoparticle internalization by the target cells,[114] and aptamers.[115]

Despite the many in-vitro therapy demonstrations using surface-modified nanoparticles, in-vivo studies have not shown widespread success in enhancing delivery. Eghtedari et al. compared PEG- and anti-HER2-PEG-coated nanorods administered to tumor-bearing mice.[116] They presented qualitative data in the form of histology to confirm that the addition of the antibody on the nanoparticle surface improved tumor accumulation. Li et al. combined gold nanorods targeted to either the HER2 or EGFR receptor and photoacoustic imaging to show that targeting enhanced the image contrast of squamous

small NANO MICRO

cell carcinoma tumor models in mice.[117] Biodistribution data were also presented showing a tumor accumulation of 6.1% of the injected dose for the nontargeted nanorods and 8.88% of the injected dose for the anti-HER2 nanorods.

Similar studies have been performed with in-vivo targeting of hollow gold nanoshells, which are ≈30 nm in diameter before surface modification. Melancon et al. modified hollow gold nanoshells with anti-EGFR and presented qualitative evidence via histology showing that the antibody-coated surface increased the delivery of nanoparticles to the tumor when compared to nonspecifically-targeted nanoparticles.[45] However, when quantitatively comparing in-vivo, anti-EGFR, hollow-gold-nanoshell tumor uptake to anti-IgG, hollow-gold-nanoshell tumor uptake using radiolabeling, the uptake difference was not statistically significant. In addition, the radiolabeling showed increased accumulation of the anti-EGFR gold nanoparticles in the liver when compared to the anti-IgG gold nanoparticles. However, another study using melanocyte-stimulating hormone (MSH) analog-modified hollow gold nanoshells to target murine melanomas showed a statistically significant enhancement of tumor delivery by targeted, hollow gold nanoshells (12.6 ± 3.1% of the injected dose per gram of tissue for the MSH-modified versus 4.3 ± 1.2% of the injected dose per gram of tissue for the nonmodified) at 4 h post-injection.[46] These results are promising, although further study is needed to conclusively determine if surface modifications of gold nanoparticles can increase tumor delivery of nanoparticles for theranostic applications.

As detailed in the following subsection, several other groups have proposed strategies involving the use of vehicles designed to carry the nanoparticles to the therapeutic site. One method is an acellular silicon microparticle that is targeted to the tumor vasculature, while another technique is cell-based, depending on the homing ability of macrophages.

For in-vivo targeting of the tumor vasculature, the use of phage technology is proposed. Bacteriophage (phage) display libraries have been used to identify peptide ligands that specifically bind the integrins, proteoglycans, and other features unique to blood vessels undergoing angiogenesis.[118] These phages can be selected and used to target tumor blood vessels for imaging or drug delivery. In addition, when coupled with gold colloidal nanospheres, gold–phage hydrogels have been imaged using darkfield microscopy, fluorescence microscopy, and NIR surface-enhanced Raman scattering spectroscopy.[119] By coating the primary particles described by Tasciotti et al. with phages specific to angiogenic blood vessels, the primary particles could be targeted to the tumor vasculature for margination, adhesion, and, ultimately, delivery of therapeutic particles. The tumor could be identified and imaged using the gold–phage hydrogel coatings of the silicon microparticles, and then treated using the delivered nanoparticles, giving these vehicles theranostic potential.

Another vehicular strategy that has been demonstrated in the literature is the aptly named "trojan horse" method (Figure 6).[121] Gold–silica nanoshells were internalized in macrophages by incubating the particles with the cells for 24 h and allowing uptake via phagocytosis. The nanoshell-loaded macrophages infiltrated tumor spheroids in vitro after 3 days of incubation and accumulated at the rim of the spheroid's core hypoxic region. Although this was not a significant enhancement of tumor core penetration, there was a marginal increase in the percentage of gold nanoparticles reaching the hypoxic core.

Although the in-vitro studies for both of these delivery strategies show some promising results, there have been no in-vivo studies delivering gold nanoparticles to date. In reality, no strategy discussed in this section has conclusively

4.2.2. Vehicles for Nanoparticle Delivery

As an alternative delivery strategy to systemic injections, a multistep delivery process has been proposed in which a large, tumor-vasculature-targeted particle carries smaller therapeutic particles to the tumor (**Figure 6**).[92] Ferrari et al. have been developing a system of 3–4 μm porous silicon particles that could be loaded with the smaller therapeutic nanoparticles, injected intravenously, and targeted to the tumor vasculature. Once the particle arrives at the tumor site and is bound, the smaller nanoparticles diffuse into the tumor. Tasciotti et al. used these porous silicon particles and demonstrated the delivery of quantum dots and single-walled carbon nanotubes to a cell's cytosol in vitro.[120] Although this system has not been applied to gold nanoparticles, it could be modified with larger pores to accommodate gold particles such as gold–gold sulfide or hollow gold nanoshells.

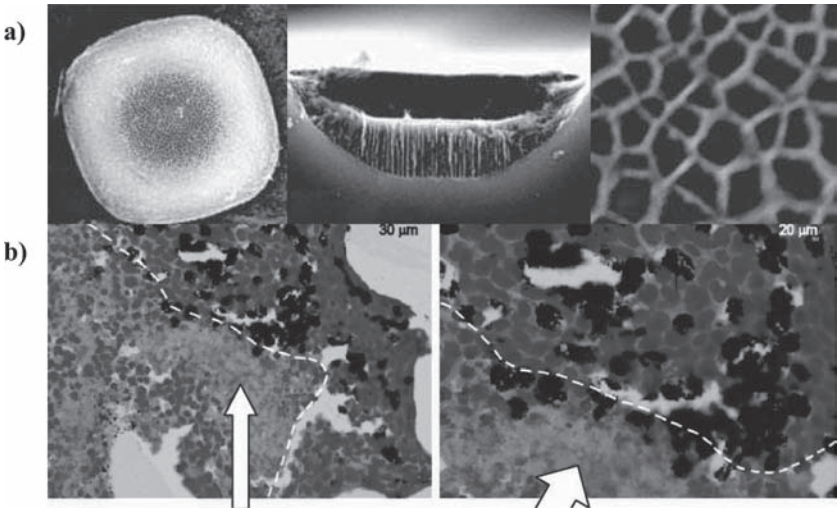

Figure 6. Delivery strategies for gold nanoparticles. a) Scanning electron microscope images of porous silicon microparticle carriers. Microparticles are loaded with therapeutic nanoparticles and targeted to the tumor vasculature. Once in the tumor vicinity, the nanoparticles locally diffuse out of the microparticle via the nanoscale pores. Reproduced with permission.[120] Copyright 2008 Nature Publishing Group. b) Hematoxylin/eosin (H&E)-stained tumor-tissue slices demonstrating the delivery of nanoparticle-laden macrophages (black cells) to the tumor. Reproduced with permission.[121] Copyright 2007 American Chemical Society.

demonstrated a significantly increased and more specific delivery of therapeutic nanoparticles to the tumor. Thus, more research is needed to more efficiently target and deliver therapeutic nanoparticles in vivo for theranostic applications.

The final area of growth that we will discuss in this paper is the study of the long-term side effects of in-vivo gold-nanoparticle presence. Determining the toxicity and side effects of gold-nanoparticle exposure is important for translating this technology to the clinical realm. Short-term studies have presented promising results, but few reports can be found in the literature exploring the effects of long-term gold accumulation throughout the body. In the next section, we will discuss the toxicity profile of gold nanoparticles.

5. Opportunity #3: Understanding Impact of Gold Nanoparticle Use In vivo

Prior to considering gold nanoparticles for any in-vivo biomedical application, it is important to understand their biocompatibility. Recent literature has suggested that nanoparticle toxicity and pharmacokinetics can depend on the size, shape, and surface charge of the particles, making surface modifications an influential factor in determining biocompatibility.[122,123] This section discusses the current understanding of gold nanoparticle cytotoxicity within the context of the differently sized, shaped, and charged gold nanoparticles studied for imaging and therapeutic applications. The first section will focus on in-vitro studies of gold nanoparticle toxicity, while the second section will discuss the in-vivo effects of gold nanoparticle administration.

5.1. Gold Nanoparticle Cytotoxicity

In-vitro cytotoxicity assays are a simple way to evaluate the basic toxicity of a material. Of the various gold nanoparticles discussed, the toxicity profile of gold colloidal nanospheres has been evaluated more extensively than the other types of gold nanoparticles. In general, gold colloidal nanospheres have induced little toxicity in vitro, with an approximate 15% reduction in cell viability observed for concentrations of 200 mg L^{-1} after 24 h.[124–126] Gold nanoparticles are typically less toxic than their metal precursors, with over 90% cell death reported after exposure to 250 μM or ≈50 mg L^{-1} of gold-salt ($AuCl_4$) solution.[127] Few studies have examined gold nanoshell or gold nanocage cytotoxicity.[6,53] Although gold nanoshells are considered biocompatible, some claim that gold nanocages or hollow gold nanoshells are more advantageous, since, without the silica core, potential silica cytotoxicity is avoided.[45]

Reports of gold nanoparticle toxicity are generally both size- and coating-dependent. For example, Pan et al. reported cytotoxicity with 1.4 nm gold nanoparticles stabilized with triphenylphosphine (half maximal inhibitory concentration (IC50) = 30–56 μM), while 15 nm triphenylphosphine-stabilized gold particles were nontoxic at 6.3 mM, suggesting that toxicity is nanoparticle-size dependent.[128] In addition, it seems that nanoparticle toxicity is also charge-dependent. Goodman et al. tested the effect of cationic (ammonium-functionalized) and anionic (carboxylate-functionalized) 2 nm gold nanoparticles at different concentrations for 24 h and found that cationic nanoparticles were more cytotoxic than the anionic.[129] Although cytotoxicity has been seen for gold nanoparticles of <5 nm at concentrations in the micromolar range, most gold nanoparticles used for therapy applications are larger than 25 nm, where the IC50 concentrations are several orders of magnitude larger. In addition, for most biological applications, the particles are PEGylated, which provides stability and protects cells from interacting with any surface detergents used to stabilize the nanoparticle.

Toxicity has been seen with gold nanorods stabilized using CTAB. Initial cytotoxicity studies of CTAB-stabilized nanorods found appreciable toxicity, which was attributed to the surface-adsorbed CTAB, a cationic detergent commonly used in nanorod synthesis.[101,130] However, Hauck et al. found that while cytotoxicity of CTAB nanorods was significant in serum-free media, the viability of cells exposed to CTAB nanorods in serum-containing media was similar to that of the control, suggesting that protein adsorption to the surface of the nanoparticles mitigated any toxic effect from the CTAB cationic surface.[16] To circumvent any potential toxicity, the CTAB must be removed. However, as a caveat to CTAB reduction, gold nanorods have demonstrated a tendency to aggregate immediately after the extraction of this surfactant.[131] Therefore, to add stability and protect against toxicity, gold nanorods are usually coated with PEG in advance of performing in-vivo applications, which reduces both cytotoxicity and nonspecific binding to cell membranes.[101] As a result, the toxicity observed from gold nanorod exposure is equal to the levels of toxicity found in other gold nanoparticles.

In addition to cell–surface interactions, gold nanoparticles can interact with the cell interior through internalization by the cell. This internalization may be desirable, particularly if the nanoparticles are designed to carry chemotherapeutics or other agents that will have a synergistic effect with thermal therapy, or if the nanoparticles are being used for photothermal-microbubble-formation therapy. Intracellular accumulation of the gold nanoparticles within a cancer cell isolates nanoparticles from healthy cells, making targeted endocytosis of gold nanoparticles by cancer cells desirable for some applications.

Gold nanoparticles have been found to easily enter cells in a size-dependent manner, most likely via receptor-mediated endocytosis. It has been observed in cell culture that the gold nanoparticle concentration in the media drops significantly within the first hour of exposure, suggesting rapid uptake of nanoparticles by cells.[127] Chithrani et al. determined the optimal particle radius for maximal cellular uptake of gold colloidal nanospheres to be ≈25 nm, with uptake ranging from 500 to 6000 particles per cell, depending on the degree of protein adsorption and the cell line used.[132] Jiang et al. also reported a similar optimal internalization size range of 25–50 nm after testing particle sizes ranging from 2 to 100 nm in diameter.[98] Using transmission electron microscopy, these particles were often found aggregated within endosomes, with few particles present in the cytosol. Controlled release of nanoparticles from endosomes for theranostic applications is an area of growing interest.

NANO MICRO small

A large number of in-vitro and in-vivo studies have indicated that gold nanoparticles have no acute or subacute toxicity on either cells or mice at the doses administered for cancer therapy. However, very little is known about the long-term effects of gold accumulation in organs such as the liver and spleen. The next subsection will focus on this topic.

5.2. In-vivo Clearance and Impact of Gold Nanoparticles

Although gold nanoparticles are often designed for prolonged circulation, clearance of the nanoparticles from the body is desired after therapy is complete. Despite evidence of renal excretion of small (<5 nm) gold nanoparticles, for larger particles several groups have reported persistence in the liver and spleen in mice for up to 6 months with no observed consequences.[100,101,106,133] Sadauskas et al. found minimal elimination of 40 nm citrate-surfaced gold nanoparticles from the liver, with an average of 16.6 μg of gold retained after 6 months, 90% of the amount measured after 24 h.[107] These studies suggest that particles may be retained in these organs permanently, as it has not been shown that gold levels return to baseline after gold nanoparticle administration. Size and surface charge may also be factors: Balogh et al. found that 46% of the initial dose of 5 nm positively charged gold–dendrimer complex particles were excreted after 5 days.[103] However, for negatively and neutrally charged 5 nm particles, as well as 11 and 22 nm particles, only ≈10% excretion of the initial dose was measured.[103]

Goodrich et al. reported the presence of foreign bodies on the liver pathology slides of 8 out of 8 animals that received intravenous injections of PEG-coated gold nanorods, and foreign bodies on the spleen pathology slides of 7 out of 8 animals.[32] These foreign bodies were hypothesized to be aggregates of gold nanorods within the tissue. They note a slow decline in the amount of gold present in the liver over the course of 28 days, while the small levels of gold detected in other organs, such as brain and kidney, remain fairly constant. Regions of chronic inflammation localized to areas where the nanorod aggregates were present were observed and rated as minimal to mild. The significance of these lesions in terms of long-term side effects is unclear from this study.

Thus far, no acute toxic effects have been observed in in-vivo studies using gold nanoparticles. However, studies to date have been limited to animal models, which are not a perfect predictor of outcomes in humans and which have also been limited to 6 months in duration. It is currently unknown if or when gold nanoparticles completely clear from the body, or if the presence of gold nanoparticles will have any undesirable consequences. To date, no detrimental effects as a result of off-target gold nanoparticle delivery have been reported, and short term toxicity studies are encouraging.

6. Conclusion

NIR-absorbing gold nanoparticles, such as gold–silica nanoshells,[6,26] gold nanorods,[33] and gold nanocages,[52,53] have shown great promise as light absorbers for cancer therapy, demonstrating an ability to destroy cancerous lesions both in vitro and in vivo. As the design of gold-nanoparticle-based thermal therapies continues to mature, efforts towards clinical translation should focus on the need for: 1) improved methods for reaching deeper, hard-to-access tumors both through alternative irradiation modalities that possess low attenuation in tissue and improved fiber-optic technologies for internal delivery of NIR light; 2) continuing progress towards modeling light–nanoparticle–tissue interactions during therapy and integration of these algorithms together with real-time imaging technologies to permit therapy optimization; 3) improved delivery methods that will allow accumulation of a larger number of particles to the tumor site, which will enhance both imaging contrast and therapy efficacy, and 4) a better grasp of the long-term consequences of gold nanoparticles remaining in organs such as the liver and spleen. With further development, gold nanoparticle therapies have the potential to improve the quality of life for subsets of cancer patients, providing a clinically viable, minimally invasive option for cancer treatment.

Acknowledgements

This work was supported in part by the Nanoscale Science and Engineering Initiative of the NSF under NSF Award Number EEC-0118007 and EEC-0647452. LCK thanks the Medical Scientist Training Program at Baylor College of Medicine and the Alliance of NanoHealth for training support. ESD and NL acknowledge support from the National Science Foundation Graduate Research Fellowship Program. AJC is supported by a National Science Foundation Graduate Research Fellowship as well as a National Defense Science and Engineering Graduate Fellowship.

[1] American Cancer Society, *Cancer Facts and Figures 2010,* American Cancer Society, Atlanta, GA **2010**.
[2] N. J. Meropol, D. Schrag, T. J. Smith, T. M. Mulvey, R. M. Langdon, D. Blum, P. A. Ubel, L. E. Schnipper, *J. Clin. Oncol.* **2009**, *27*, 3868.
[3] J. Aaseth, M. Haugen, O. Forre, *Analyst* **1998**, *123*, 3.
[4] I. H. El-Sayed, X. Huang, M. A. El-Sayed, *Nano Lett.* **2005**, *5*, 829.
[5] C. Loo, L. Hirsch, M. H. Lee, E. Chang, J. West, N. Halas, R. Drezek, *Opt. Lett.* **2005**, *30*, 1012.
[6] L. R. Hirsch, R. J. Stafford, J. A. Bankson, S. R. Sershen, B. Rivera, R. E. Price, J. D. Hazle, N. J. Halas, J. L. West, *Proc. Natl. Acad. Sci. USA* **2003**, *100*, 13549.
[7] A. M. Gobin, M. H. Lee, N. J. Halas, W. D. James, R. A. Drezek, J. L. West, *Nano Lett.* **2007**, *7*, 1929.
[8] J. L. Li, L. Wang, X. Y. Liu, Z. P. Zhang, H. C. Guo, W. M. Liu, S. H. Tang, *Cancer Lett.* **2009**, *274*, 319.
[9] Pilot Study of AuroLase Therapy in Refractory and/or Recurrent Tumors of the Head and Neck, http://clinicaltrials.gov/ct2/show/NCT00848042 (accessed September 2010).
[10] R. K. Jain, *Annu. Rev. Biomed. Eng.* **1999**, *1*, 241.
[11] C. J. Gannon, C. R. Patra, R. Bhattacharya, P. Mukherjee, S. A. Curley, *J. Nanobiotechnol.* **2008**, *6*, 2.

[12] M. Johannsen, U. Gneveckow, L. Eckelt, A. Feussner, N. Waldofner, R. Scholz, S. Deger, P. Wust, S. A. Loening, A. Jordan, *Int. J. Hyperthermia* **2005**, *21*, 637.
[13] L. Tong, Y. Zhao, T. B. Huff, M. N. Hansen, A. Wei, J. X. Cheng, *Adv. Mater. Deerfield* **2007**, *19*, 3136.
[14] L. B. Carpin, L. R. Bickford, G. Agollah, T. K. Yu, R. Schiff, Y. Li, R. A. Drezek, *Breast Cancer Res. Treat.*, DOI: 10.1007/s10549-010-0811-5.
[15] P. Diagaradjane, A. Shetty, J. C. Wang, A. M. Elliott, J. Schwartz, S. Shentu, H. C. Park, A. Deorukhkar, R. J. Stafford, S. H. Cho, J. W. Tunnell, J. D. Hazle, S. Krishnan, *Nano Lett.* **2008**, *8*, 1492.
[16] T. S. Hauck, T. L. Jennings, T. Yatsenko, J. C. Kumaradas, W. C. W. Chan, *Adv. Mater.* **2008**, *20*, 3832.
[17] L. Bickford, J. Sun, K. Fu, N. Lewinski, V. Nammalvar, J. Chang, R. Drezek, *Nanotechnology* **2008**, *19*, 315102.
[18] J. Park, A. Estrada, K. Sharp, K. Sang, J. A. Schwartz, D. K. Smith, C. Coleman, J. D. Payne, B. A. Korgel, A. K. Dunn, J. W. Tunnell, *Opt. Express* **2008**, *16*, 1590.
[19] L. R. Bickford, G. Agollah, R. Drezek, T. K. Yu, *Breast Cancer Res. Treat.* **2010**, *120*, 547.
[20] C. Loo, A. Lin, L. Hirsch, M. H. Lee, J. Barton, N. Halas, J. West, R. Drezek, *Technol. Cancer Res. Treat.* **2004**, *3*, 33.
[21] A. R. Lowery, A. M. Gobin, E. S. Day, N. J. Halas, J. L. West, *Int. J. Nanomedicine* **2006**, *1*, 149.
[22] A. M. Gobin, J. J. Moon, J. L. West, *Int. J. Nanomedicine* **2008**, *3*, 351.
[23] J. M. Stern, J. Stanfield, Y. Lotan, S. Park, J. T. Hsieh, J. A. Cadeddu, *J. Endourol.* **2007**, *21*, 939.
[24] R. J. Bernardi, A. R. Lowery, P. A. Thompson, S. M. Blaney, J. L. West, *J. Neurooncol.* **2008**, *86*, 165.
[25] S. Y. Liu, Z. S. Liang, F. Gao, S. F. Luo, G. Q. Lu, *J. Mater. Sci. Mater. Med.* **2010**, *21*, 665.
[26] D. P. O'Neal, L. R. Hirsch, N. J. Halas, J. D. Payne, J. L. West, *Cancer Lett.* **2004**, *209*, 171.
[27] J. A. Schwartz, A. M. Shetty, R. E. Price, R. J. Stafford, J. C. Wang, R. K. Uthamanthil, K. Pham, R. J. McNichols, C. L. Coleman, J. D. Payne, *Cancer Res.* **2009**, *69*, 1659.
[28] J. R. Cole, N. A. Mirin, M. W. Knight, G. P. Goodrich, N. J. Halas, *J. Phys. Chem. C* **2009**, *113*, 12090.
[29] P. K. Jain, K. S. Lee, I. H. El-Sayed, M. A. El-Sayed, *J. Phys. Chem. B* **2006**, *110*, 7238.
[30] G. von Maltzahn, J. H. Park, A. Agrawal, N. K. Bandaru, S. K. Das, M. J. Sailor, S. N. Bhatia, *Cancer Res.* **2009**, *69*, 3892.
[31] E. B. Dickerson, E. C. Dreaden, X. Huang, I. H. El-Sayed, H. Chu, S. Pushpanketh, J. F. McDonald, M. A. El-Sayed, *Cancer Lett.* **2008**, *269*, 57.
[32] G. P. Goodrich, L. Bao, K. Gill-Sharp, K. L. Sang, J. Wang, J. D. Payne, *J. Biomed. Opt.* **2010**, *15*, 018001.
[33] X. Huang, I. H. El-Sayed, W. Qian, M. A. El-Sayed, *J. Am. Chem. Soc.* **2006**, *128*, 2115.
[34] N. J. Durr, T. Larson, D. K. Smith, B. A. Korgel, K. Sokolov, A. Ben-Yakar, *Nano Lett.* **2007**, *7*, 941.
[35] C. L. Didychuk, P. Ephrat, A. Chamson-Reig, S. L. Jacques, J. J. L. Carson, *Nanotechnology* **2009**, *20*, 195102.
[36] J. W. M. Chon, C. Bullen, P. Zijlstra, M. Gu, *Adv. Funct. Mater.* **2007**, *17*, 875.
[37] P. Zijlstra, J. W. M. Chon, M. Gu, *Opt. Express* **2007**, *15*, 12151.
[38] Y. Horiguchi, K. Honda, Y. Kato, N. Nakashima, Y. Niidome, *Langmuir* **2008**, *24*, 12026.
[39] G. Raschke, S. Brogl, A. S. Susha, A. L. Rogach, T. A. Klar, J. Feldmann, B. Fieres, N. Petkov, T. Bein, A. Nichtl, K. Kuerzinger, *Nano Lett.* **2005**, *5*, 811.
[40] A. M. Schwartzberg, C. D. Grant, T. van Buuren, J. Z. Zhang, *J. Phys. Chem. C* **2007**, *111*, 8892.
[41] J. Z. Zhang, A. M. Schwartzberg, J. Norman, T. C. D. Grant, J. Liu, F. Bridges, T. van Buuren, *Nano Lett.* **2005**, *5*, 809.
[42] A. M. Gobin, E. M. Watkins, E. Quevedo, V. L. Colvin, J. L. West, *Small* **2010**, *6*, 745.
[43] B. G. Prevo, S. A. Esakoff, A. Mikhailovsky, J. A. Zasadzinski, *Small* **2008**, *4*, 1183.
[44] A. M. Schwartzberg, T. Y. Olson, C. E. Talley, J. Z. Zhang, *J. Phys. Chem. B* **2006**, *110*, 19935.
[45] M. P. Melancon, W. Lu, Z. Yang, R. Zhang, Z. Cheng, A. M. Elliot, J. Stafford, T. Olson, J. Z. Zhang, C. Li, *Mol. Cancer Ther.* **2008**, *7*, 1730.
[46] W. Lu, C. Xiong, G. Zhang, Q. Huang, R. Zhang, J. Z. Zhang, C. Li, *Clin. Cancer Res.* **2009**, *15*, 876.
[47] R. Kumar, A. N. Maitra, P. K. Patanjali, P. Sharma, *Biomaterials* **2005**, *26*, 6743.
[48] S. E. Skrabalak, J. Chen, Y. Sun, X. Lu, L. Au, C. M. Cobley, Y. Xia, *Acc. Chem. Res.* **2008**, *41*, 1587.
[49] J. Chen, F. Saeki, B. J. Wiley, H. Cang, M. J. Cobb, Z. Y. Li, L. Au, H. Zhang, M. B. Kimmey, X. Li, Y. Xia, *Nano Lett.* **2005**, *5*, 473.
[50] L. Au, D. Zheng, F. Zhou, Z. Y. Li, X. Li, Y. Xia, *ACS Nano* **2008**, *2*, 1645.
[51] J. Chen, D. Wang, J. Xi, L. Au, A. Siekkinen, A. Warsen, Z. Y. Li, H. Zhang, Y. Xia, X. Li, *Nano Lett.* **2007**, *7*, 1318.
[52] S. E. Skrabalak, J. Chen, L. Au, X. Lu, X. Li, Y. Xia, *Adv. Mater. Deerfield* **2007**, *19*, 3177.
[53] J. Chen, C. Glaus, R. Laforest, Q. Zhang, M. Yang, M. Gidding, M. J. Welch, Y. Xia, *Small* **2010**, *6*, 811.
[54] G. T. Boyd, Z. H. Yu, Y. R. Shen, *Phys. Rev. B—Condens. Matter* **1986**, *33*, 7923.
[55] K. Sokolov, M. Follen, J. Aaron, I. Pavlova, A. Malpica, R. Lotan, R. Richards-Kortum, *Cancer Res.* **2003**, *63*, 1999.
[56] M. Abdulla-Al-Mamun, Y. Kusumoto, A. Mihata, M. S. Islam, B. Ahmmad, *Photochem. Photobiol. Sci.* **2009**, *8*, 1125.
[57] I. H. El-Sayed, X. Huang, M. A. El-Sayed, *Cancer Lett.* **2006**, *239*, 129.
[58] X. Huang, W. Qian, I. H. El-Sayed, M. A. El-Sayed, *Lasers Surg. Med.* **2007**, *39*, 747.
[59] V. P. Zharov, E. N. Galitovskaya, C. Johnson, T. Kelly, *Lasers Surg. Med.* **2005**, *37*, 219.
[60] D. Lapotko, E. Lukianova, M. Potapnev, O. Aleinikova, A. Oraevsky, *Cancer Lett.* **2006**, *239*, 36.
[61] D. O. Lapotko, E. Lukianova, A. A. Oraevsky, *Lasers Surg. Med.* **2006**, *38*, 631.
[62] D. O. Lapotko, *Lasers Surg. Med.* **2006**, *38*, 240.
[63] C. F. Bohren, D. R. Huffman, *Absorption and Scattering of Light by Small Particles*, Wiley, New York **1983**.
[64] H. C. van de Hulst, *Light Scattering by Small Particles*, Wiley, New York **1957**.
[65] P. K. Jain, K. S. Lee, I. H. El-Sayed, M. A. El-Sayed, *J. Phys. Chem. B* **2006**, *110*, 7238.
[66] C. Noguez, *J. Phys. Chem. C* **2007**, *111*, 3806.
[67] N. Harris, M. J. Ford, M. B. Cortie, *J. Phys. Chem. B* **2006**, *110*, 10701.
[68] W. C. Dewey, *Int. J. Hyperthermia* **1994**, *10*, 457.
[69] R. W. Habash, R. Bansal, D. Krewski, H. T. Alhafid, *Crit. Rev. Biomed. Eng.* **2006**, *34*, 459.
[70] B. Hildebrandt, P. Wust, O. Ahlers, A. Dieing, G. Sreenivasa, T. Kerner, R. Felix, H. Riess, *Crit. Rev. Oncol. Hematol.* **2002**, *43*, 33.
[71] X. Huang, P. K. Jain, I. H. El-Sayed, M. A. El-Sayed, *Photochem. Photobiol.* **2006**, *82*, 412.
[72] R. Weissleder, *Nat. Biotechnol.* **2001**, *19*, 316.
[73] R. Weissleder, V. Ntziachristos, *Nat. Med.* **2003**, *9*, 123.
[74] J. Vera, Y. Bayazitoglu, *Int. J. Heat Mass Tran.* **2009**, *52*, 3402.
[75] A. Elliott, J. Schwartz, J. Wang, A. Shetty, J. Hazle, J. R. Stafford, *Lasers Surg. Med.* **2008**, *40*, 660.
[76] A. M. Elliott, J. Schwartz, J. Wang, A. M. Shetty, C. Bourgoyne, D. P. O'Neal, J. D. Hazle, R. J. Stafford, *Medical Physics* **2009**, *36*, 1351.

[77] A. M. Elliott, R. J. Stafford, J. Schwartz, J. Wang, A. M. Shetty, C. Bourgoyne, P. O'Neal, J. D. Hazle, *Medical Physics* **2007**, *34*, 3102.
[78] J. Vera, Y. Bayazitoglu, *Int. J. Heat Mass Tran.* **2009**, *52*, 564.
[79] P. Puvanakrishnan, J. Park, P. Diagaradjane, J. A. Schwartz, C. L. Coleman, K. L. Gill-Sharp, K. L. Sang, J. D. Payne, S. Krishnan, J. W. Tunnell, *J. Biomed. Opt.* **2009**, *14*, 024044.
[80] J. P. McGhana, G. D. Dodd, *AJR Am. J. Roentgenol.* **2001**, *176*, 3.
[81] P. Bernardi, M. Cavagnaro, S. Pisa, E. Piuzzi, *IEEE Trans. Biomed. Eng.* **2003**, *50*, 295.
[82] J. Cardinal, J. R. Klune, E. Chory, G. Jeyabalan, J. S. Kanzius, M. Nalesnik, D. A. Geller, *Surgery* **2008**, *144*, 125.
[83] C. J. Gannon, P. Cherukuri, B. I. Yakobson, L. Cognet, J. S. Kanzius, C. Kittrell, R. B. Weisman, M. Pasquali, H. K. Schmidt, R. E. Smalley, S. A. Curley, *Cancer* **2007**, *110*, 2654.
[84] Q. A. Pankhurst, J. Connolly, S. K. Jones, J. Dobson, *J. Phys. D—Appl. Phys.* **2003**, *36*, 167.
[85] K. Maier-Hauff, R. Rothe, R. Scholz, U. Gneveckow, P. Wust, B. Thiesen, A. Feussner, A. von Deimling, N. Waldoefner, R. Felix, A. Jordan, *J. Neurooncol.* **2007**, *81*, 53.
[86] T. A. Larson, J. Bankson, J. Aaron, K. Sokolov, *Nanotechnology* **2007**, *18*, 325101.
[87] C. S. Levin, C. Hofmann, T. A. Ali, A. T. Kelly, E. Morosan, P. Nordlander, K. H. Whitmire, N. J. Halas, *ACS Nano* **2009**.
[88] A. Wijaya, K. A. Brown, J. D. Alper, K. Hamad-Schifferli, *J. Magn. Magn. Mater.* **2007**, *309*, 15.
[89] Z. Xu, Y. Hou, S. Sun, *J. Am. Chem. Soc.* **2007**, *129*, 8698.
[90] D. K. Kirui, D. A. Rey, C. A. Batt, *Nanotechnology* **2010**, *21*, 105105.
[91] J. Shah, S. Park, S. Aglyamov, T. Larson, L. Ma, K. Sokolov, K. Johnston, T. Milner, S. Y. Emelianov, *J. Biomed. Opt.* **2008**, *13*.
[92] P. Decuzzi, R. Pasqualini, W. Arap, M. Ferrari, *Pharm. Res.* **2009**, *26*, 235.
[93] J. M. Harris, R. B. Chess, *Nat. Rev. Drug Discov.* **2003**, *2*, 214.
[94] M. J. Roberts, M. D. Bentley, J. M. Harris, *Adv. Drug Deliver. Rev.* **2002**, *54*, 459.
[95] G. D. Zhang, Z. Yang, W. Lu, R. Zhang, Q. Huang, M. Tian, L. Li, D. Liang, C. Li, *Biomaterials* **2009**, *30*, 1928.
[96] G. S. Terentyuk, G. N. Maslyakova, L. V. Suleymanova, B. N. Khlebtsov, B. Y. Kogan, G. G. Akchurin, A. V. Shantrocha, I. L. Maksimova, N. G. Khlebtsov, V. V. Tuchin, *J. Biophotonics* **2009**, *2*, 292.
[97] S. D. Perrault, C. Walkey, T. Jennings, H. C. Fischer, W. C. Chan, *Nano Lett.* **2009**, *9*, 1909.
[98] W. Jiang, B. Y. S. Kim, J. T. Rutka, W. C. W. Chan, *Nat. Nanotechnol.* **2008**, *3*, 145.
[99] B. Kim, G. Han, B. J. Toley, C. K. Kim, V. M. Rotello, N. S. Forbes, *Nat. Nanotechnol.* **2010**, *5*, 465.
[100] W. D. James L. R. Hirsch, J. L. West, P. D. O'Neal, J. D. Payne, *J. Radioanal. Nucl. Ch.* **2007**, *271*, 455.
[101] T. Niidome, M. Yamagata, Y. Okamoto, Y. Akiyama, H. Takahashi, T. Kawano, Y. Katayama, Y. Niidome, *J. Control. Release* **2006**, *114*, 343.
[102] Y. Akiyama, T. Mori, Y. Katayama, T. Niidome, *J. Control. Release* **2009**, *139*, 81.
[103] L. Balogh, S. S. Nigavekar, B. M. Nair, W. Lesniak, C. Zhang, L. Y. Sung, M. S. T. Kariapper, A. El-Jawahri, M. Llanes, B. Bolton, F. Mamou, W. Tan, A. Hutson, L. Minc, M. K. Khan, *Nanomed.—Nanotechnol.* **2007**, *3*, 281.
[104] W. S. Cho, M. J. Cho, J. Jeong, M. Choi, H. Y. Cho, B. S. Han, S. H. Kim, H. O. Kim, Y. T. Lim, B. H. Chung, J. Jeong, *Toxicol. Appl. Pharm.* **2009**, *236*, 16.
[105] W. H. De Jong, W. I. Hagens, P. Krystek, M. C. Burger, A. J. A. M. Sips, R. E. Geertsma, *Biomaterials* **2008**, *29*, 1912.
[106] X. L. Huang, B. Zhang, L. Ren, S. F. Ye, L. P. Sun, Q. Q. Zhang, M. C. Tan, G. M. Chow, *J. Mater. Sci.—Mater. M.* **2008**, *19*, 2581.
[107] E. Sadauskas, G. Danscher, M. Stoltenberg, U. Vogel, A. Larsen, H. Wallin, *Nanomedicine* **2009**, *5*, 162.
[108] J. M. Stern, J. Stanfield, W. Kabbani, J. T. Hsieh, J. R. A. Cadeddu, *J. Urology* **2008**, *179*, 748.
[109] E. Sadauskas, H. Wallin, M. Stoltenberg, U. Vogel, P. Doering, A. Larsen, G. Danscher, *Part. Fibre Toxicol.* **2007**, *4*, 10.
[110] C. Loo, A. Lowery, N. Halas, J. West, R. Drezek, *Nano Lett.* **2005**, *5*, 709.
[111] R. S. Norman, J. W. Stone, A. Gole, C. J. Murphy, T. L. Sabo-Attwood, *Nano Lett.* **2008**, *8*, 302.
[112] K. C. Black, N. D. Kirkpatrick, T. S. Troutman, L. Xu, J. Vagner, R. J. Gillies, J. K. Barton, U. Utzinger, M. Romanowski, *Mol. Imaging* **2008**, *7*, 50.
[113] N. Chanda, R. Shukla, K. V. Katti, R. Kannan, *Nano Lett.* **2009**, *9*, 1798.
[114] L. Sun, D. Liu, Z. Wang, *Langmuir* **2008**, *24*, 10293.
[115] Y. F. Huang, K. Sefah, S. Bamrungsap, H. T. Chang, W. Tan, *Langmuir* **2008**, *24*, 11860.
[116] M. Eghtedari, A. V. Liopo, J. A. Copland, A. A. Oraevslty, M. Motamedi, *Nano Lett.* **2009**, *9*, 287.
[117] P. C. Li, C. R. Wang, D. B. Shieh, C. W. Wei, C. K. Liao, C. Poe, S. Jhan, A. A. Ding, Y. N. Wu, *Opt. Express* **2008**, *16*, 18605.
[118] E. Ruoslahti, *Semin. Cancer Biol.* **2000**, *10*, 435.
[119] G. R. Souza, D. R. Christianson, F. I. Staquicini, M. G. Ozawa, E. Y. Snyder, R. L. Sidman, J. H. Miller, W. Arap, R. Pasqualini, *Proc. Natl. Acad. Sci. USA* **2006**, *103*, 1215.
[120] E. Tasciotti, X. Liu, R. Bhavane, K. Plant, A. D. Leonard, B. K. Price, M. M. Cheng, P. Decuzzi, J. M. Tour, F. Robertson, M. Ferrari, *Nat. Nanotechnol.* **2008**, *3*, 151.
[121] M. R. Choi, K. J. Stanton-Maxey, J. K. Stanley, C. S. Levin, R. Bardhan, D. Akin, S. Badve, J. Sturgis, J. P. Robinson, R. Bashir, N. J. Halas, S. E. Clare, *Nano Lett.* **2007**, *7*, 3759.
[122] N. Lewinski, V. Colvin, R. Drezek, *Small* **2008**, *4*, 26.
[123] C. J. Murphy, A. M. Gole, J. W. Stone, P. N. Sisco, A. M. Alkilany, E. C. Goldsmith, S. C. Baxter, *Acc. Chem. Res.* **2008**, *41*, 1721.
[124] A. K. Salem, P. C. Searson, K. W. Leong, *Nat. Mater.* **2003**, *2*, 668.
[125] D. Shenoy, W. Fu, J. Li, C. Crasto, G. Jones, C. DiMarzio, S. Sridhar, M. Amiji, *Int. J. Nanomed.* **2006**, *1*, 51.
[126] C. H. Su, H. S. Sheu, C. Y. Lin, C. C. Huang, Y. W. Lo, Y. C. Pu, J. C. Weng, D. B. Shieh, J. H. Chen, C. S. Yeh, *J. Am. Chem. Soc.* **2007**, *129*, 2139.
[127] E. E. Connor, J. Mwamuka, A. Gole, C. J. Murphy, M. D. Wyatt, *Small* **2005**, *1*, 325.
[128] Y. Pan, S. Neuss, A. Leifert, M. Fischler, F. Wen, U. Simon, G. Schmid, W. Brandau, W. Jahnen-Dechent, *Small* **2007**, *3*, 1941.
[129] C. M. Goodman, C. D. McCusker, T. Yilmaz, V. M. Rotello, *Bioconjugate Chem.* **2004**, *15*, 897.
[130] T. B. Huff, M. N. Hansen, Y. Zhao, J. X. Cheng, A. Wei, *Langmuir* **2007**, *23*, 1596.
[131] H. Liao, J. Hafner, *Chem. Mater.* **2005**, *17*, 4636.
[132] B. D. Chithrani, A. A. Ghazani, W. C. W. Chan, *Nano Lett.* **2006**, *6*, 662.
[133] J. F. Hainfeld, D. N. Slatkin, T. M. Focella, H. M. Smilowitz, *Brit. J. Radiol.* **2006**, *79*, 248.

Received: January 28, 2010
Revised: April 6, 2010
Published online:

